CHIN. PHYS. LETT. Vol. 32, No. 4 (2015) 043202

Generation of Linear Isolated Sub-60 Attosecond Pulses by Combining a Circularly Polarized Pulse with an Elliptically Polarized Pulse *

XIA Chang-Long(夏昌龙), MIAO Xiang-Yang(苗向阳)**

College of Physics and Information Engineering, Shanxi Normal University, Linfen 041004

(Received 22 December 2014)

The two-color circularly polarized pulses scheme was proposed to generate isolated attosecond pulses in our previous work [Phys. Rev. A 87 (2013) 043406], while the polarization of the attosecond pulse was not investigated. We show a supplementary explanation of this scheme and present another scheme to generate linear isolated attosecond pulses by combining a circularly polarized pulse with an elliptically polarized pulse. High-order harmonic generation and quantum path control are investigated to compare these two schemes. Both schemes can obtain supercontinuum spectra plateau from about 200 eV to 550 eV, which belong to the water window region. It is found that the latter scheme can clearly eliminate the short quantum path and extend the harmonic plateau. A linear isolated attosecond pulse with a duration of sub-60 as can be generated by superposing a bandwidth of 70 eV.

PACS: 32.80.Rm, 42.65.Ky DOI: 10.1088/0256-307X/32/4/043202

Research of isolated attosecond pulses (IAPs) has been a hot subject in ultrafast science due to their important applications,[1–4] such as tracing the bound electron motion in atoms and molecules,[5] Auger decay,[6] and other phenomena in attosecond time scale.[7] Recently, IAPs are mainly obtained by superposing several orders of high-order harmonic spectra in experiments.[8,9] High-order harmonics generate twice in one optical cycle due to the symmetry of the incident laser pulse.[10] The interference between quantum paths generates modulation on the high-order harmonic spectrum and creates attosecond trains, while IAPs are more useful in ultrafast physics than in attosecond pulse trains. Thus, controlling the quantum path is one point to generate IAPs.[11,12] From the uncertain relation $\Delta E \Delta T \geq \hbar/2$, it is known that a longer bandwidth may lead to a short duration, thus IAP generation also needs a broad supercontinuum spectrum of high-order harmonic generation (HHG). The bandwidth from 280 eV to 550 eV corresponding to the wavelength from 2.3 nm to 4.4 nm, which is called water window, has more applications in detecting with ultrafast time resolution, especially in detecting the imaging of live cells.[13,14] Due to the fact that the ponderomotive potential is proportional to $I\lambda^2$, higher intensity and longer wavelength may obtain broader plateau of HHG.[15] We use a midinfrared laser pulse to obtain the HHG that includes the water window region.

Various schemes have been introduced to obtain IAPs, such as the few-cycle scheme,[16] ionization gating,[17] polarization gating (PG),[18] and the two-color field scheme.[19–21] In addition, an isolated attosecond pulse with the duration of 67 as was obtained by the double optical gating (DOG) in experiment,[22] which is the shortest duration to our best knowledge. The PG scheme usually combines two counterrotating pulses, and the DOG scheme adds another pulse to a PG technique. The frequencies of the two circularly polarized pulses in the PG and DOG schemes are the same.[8,18] We investigated the IAP generation from two-color circularly polarized pulses (circularly polarized pulse combing with another circularly polarized pulse, i.e., CC scheme), and found that when the frequencies of the two circularly polarized pulses are different, the 'gating' structure in PG will disappear and the quantum paths will be controlled.[23] Much attention has been paid to the polarization of the attosecond pulse in atoms and molecules.[24] Controlling the polarization of an attosecond pulse train was proposed by a two-color field of orthogonally polarized pulses.[25] Du *et al.* investigated the elliptically polarized IAP generation from the $2p_0$ state of He^+ by two color fields of linearly polarized pulses.[26] However, the polarization of the attosecond pulse was not investigated in the CC scheme. Here, an explanation of the polarization of the CC scheme is supplemented and a left circularly polarized pulse scheme combined with a right elliptically polarized pulse scheme (i.e., CE scheme) is explored to obtain IAPs. In addition, the polarization of the attosecond pulse is also investigated. The CE scheme can control the ellipticity while

*Supported by the National Natural Science Foundation of China under Grant Nos 11404204 and 11447208, the Key Project of Chinese Ministry of Education under Grant No 211025, the Research Fund for the Doctoral Program of Higher Education of China under Grant No 20111404120004, and the Natural Science Foundation for Young Scientists of Shanxi Province under Grant No 2009021005.

**Corresponding author. Email: sxxymiao@126.com

© 2015 Chinese Physical Society and IOP Publishing Ltd

the CC scheme cannot, which is beneficial to control the HHG and to generate IAPs. These schemes can be used to refit the DOG equipment by adding an optical device, such as a doubling crystal.

In this Letter, we numerically solve the time-dependent Schrödinger equation (in atomic units)

$$i\frac{\partial\Psi(x,y,t)}{\partial t} = \Big[\frac{p_x^2+p_y^2}{2} + V(x,y) + xE_x(t) + yE_y(t)\Big]\Psi(x,y,t), \quad (1)$$

where $V(x,y) = -q/\sqrt{x^2+y^2+a^2}$ is a two-dimensional soft-core Coulomb potential. In our simulation, $q = 1.5$ and $a^2 = 0.6$, which correspond to the binding energy of 0.9 a.u. for the ground state of a helium atom. $E(t) = \hat{x}E_x(t) + \hat{y}E_y(t)$ is the combination field and is generated by a left circularly polarized pulse and a right elliptically polarized pulse. The details of the two electric fields are as follows:

$$\begin{aligned}\boldsymbol{E}_{\rm cir}(t) &= E_0 f(t - T_{\rm d}/2)[\hat{x}\cos(\omega_1 t) + \hat{y}\sin(\omega_1 t)],\\ \boldsymbol{E}_{\rm ellip}(t) &= E_0 f(t + T_{\rm d}/2)\Big[\hat{x}\frac{1}{\sqrt{(1+\varepsilon^2)}}\cos(\omega_2 t + \pi/2)\\ &\quad - \hat{y}\frac{\varepsilon}{\sqrt{(1+\varepsilon^2)}}\sin(\omega_2 t + \pi/2)\Big]. \quad (2)\end{aligned}$$

Thus, the x- and y-component field (i.e., E_x and E_y) can be obtained by superposing Eqs. (2) and (3).

Here $f(t) = \exp[-2\ln(2)t^2/\tau^2]$, $\tau = 7$ fs, $T_{\rm d} = 5$ fs and $\omega_{1,2}$ are the envelope, pulse duration, time delay, and the frequencies of the laser pulses, respectively, and ε is the ellipticity of the right elliptically pulse.

In our calculation, the laser parameters are set as $\omega_1 = 0.04286$ and $\omega_2 = 0.0285$, which correspond to the wavelengths 1064 nm and 1600 nm. Both intensities in two pulses are $I_0 = 6\times10^{14}$ W/cm^2. First, we calculate the HHG with different ellipticities of the elliptically polarized pulse. Figure 1(a) shows the CC scheme and the CE scheme, i.e., $\varepsilon = 1.0$ and $\varepsilon = 0.9$. Supercontinuum plateaus of HHG are obtained for both of the cases. The cutoff is 550 eV for the case of $\varepsilon = 0.9$, which is higher than 530 eV for the case of $\varepsilon = 1.0$. Thus, the CE scheme can extend the HHG spectrum. In addition, the multiplateau structure of HHG is obtained, which is due to the coherence of different emission events.[15] We try to change the ellipticity to make it smaller, i.e., $\varepsilon = 0.7$ and $\varepsilon = 0.5$, as shown in Fig. 1(b). The cutoffs are 590 eV and 650 eV for the two cases. This implies that the harmonic plateau of HHG broadens as the ellipticity reduces. From Fig. 1(b), it is found that lower ellipticity may lead to more modulations in the plateau of HHG, which is not conducive to obtaining IAPs. All of the above HHG spectra have a supercontinuum plateau with a bandwidth longer than 280 eV, which is in the water window region. The intensity of HHG is low, which is due to fact that the wavelength of the laser pulse is long. This decrease can be balanced by favorable phase matching at high pressure.[27] We take the case of $\varepsilon = 0.7$ and $\varepsilon = 1.0$ in the following to discuss the quantum path for the cases of the CE and CC schemes.

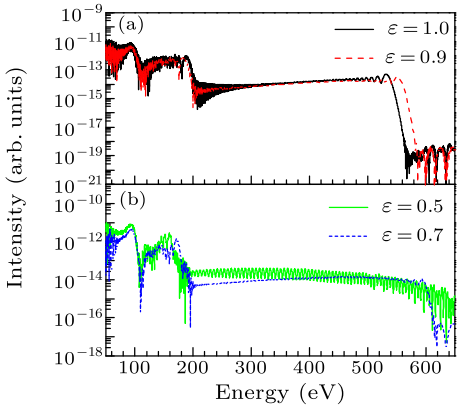

Fig. 1. The HHG spectrum obtained with different ellipticities: (a) $\varepsilon = 1.0$ and $\varepsilon = 0.9$ shown in black solid and red dashed lines; (b) $\varepsilon = 0.7$ and $\varepsilon = 0.5$ shown in green solid and blue dotted lines.

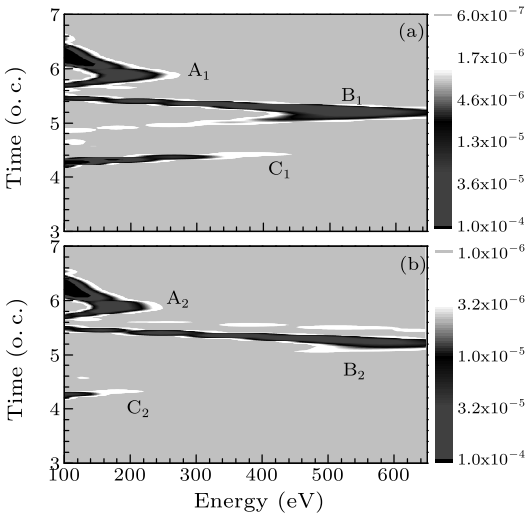

Fig. 2. Time frequency profiles for (a) the CC scheme and (b) the CE scheme with ellipticity 0.7.

Secondly, we present the calculation for the time-frequency analysis to discuss the quantum paths that are responsible to the HHG. Figure 2(a) shows the case of the CC scheme, and the parameters are the same as the black solid line shown in Fig. 1(a). Three energy peaks contribute to the plateau area of HHG, which are marked as A_1, B_1 and C_1. The energies of peaks A_1 and C_1 are about 205 eV and the energy of peak B_1 is 530 eV, these results correspond to the multiplateau cutoffs of HHG. The intensity of the short path is much weaker than that of the long path in the quantum peak B_1, thus the interference between two paths is weak. This can explain the structure of supercontin-

uum plateau shown in the HHG spectrum. Figure 2(b) shows the case of the CE scheme, i.e., $\varepsilon = 0.7$. There are also three energy peaks, the intensity of peak C_2 is much weaker than that of other two peaks. The energies of peaks A_2 and B_2 are about 200 eV and 590 eV, which correspond to the HHG spectrum. The electron obtains different energies at different emission optical cycles in the laser field with Gaussian envelopes. This leads to the generation of the multiplateau structure. By comparing the CC scheme with the CE scheme, it can be seen that the intensity of peak C_2 is weaker than that of peak C_1. Only long path in peak B_2 contributes to HHG for the case of the CE scheme, while a weaker short path emerges in peak B_1 for the case of the CC scheme. In other words, the CE scheme can control the short path responsible to the plateau of HHG, which is helpful to obtain IAPs directly by superposing a bandwidth in a plateau area.

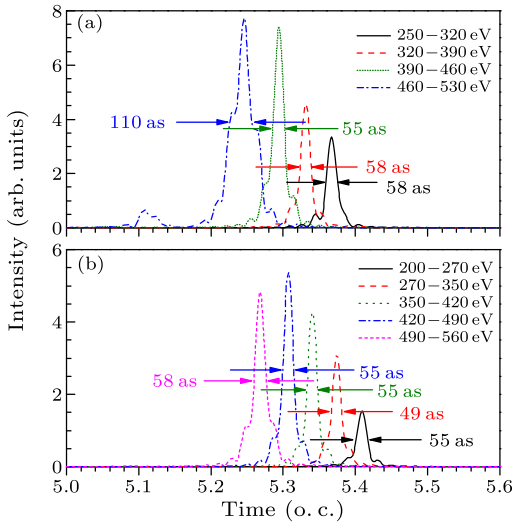

Fig. 3. IAP generation by superposing a bandwidth of 70 eV: (a) for the case of the CC scheme, 250–320 eV, 320–390 eV, 390–460 eV and 460–530 eV, shown in black solid line, red dashed line, green dotted line and blue dash-dotted line, respectively; (b) for the case of $\varepsilon = 0.7$, 200–270 eV, 270–350 eV, 350–420 eV, 420–490 eV and 490–560 eV, shown in black solid line, red dashed line, green dotted line and blue dash-dotted line and magenta short dashed line, respectively.

Next, by superposing a bandwidth of 70 eV in the plateau region, we calculate temporal envelopes of attosecond pulse generation. For the case of the CC scheme, attosecond pulses form the regions 250–320 eV, 320–390 eV, 390–460 eV and 460–530 eV, as shown in Fig. 3(a), and the full widths at half-maximum (FWHM) are 58 as, 58 as, 55 as and 110 as, respectively. The intensity of the attosecond pulse increases as the region moves to cutoff. This is due to the fact that the intensity of the quantum path is lower at a smaller value of energy in peak B_1. For the case of 460–530 eV, a small satellite pulse appears and the FWHM is twice as wide as the others. This is in agreement with the short quantum path in peak B_1 that turns stronger near the cutoff area. For the case of the CE scheme (i.e., $\varepsilon = 0.7$), isolated attosecond pulses with FWHMs of 55 as, 49 as, 55 as, 55 as, and 58 as are obtained by superposing the regions 200–270 eV, 270–350 eV, 350–420 eV, 420–490 eV and 490–560 eV, respectively. The generation time and the intensity of these attosecond pulses are in good agreement with the results shown in Fig. 2. The IAP with the FWHM of sub-60 as can be generated in the plateau area for the two cases and the central wavelength is selectable in the water window region.

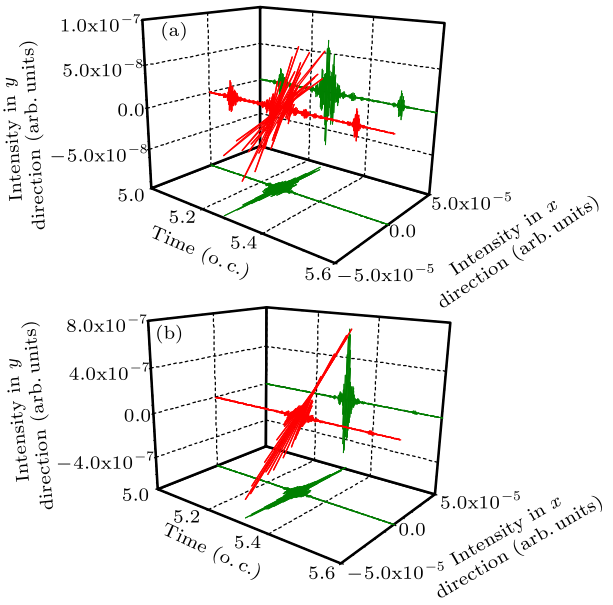

Fig. 4. Electric field of attosecond pulse in a 3D coordinate system: (a) the CC scheme, by superposing the region 390–460 eV, (b) the CE scheme, by superposing the region 420–490 eV.

Lastly, we calculate the electric fields of the attosecond pulse in the 3D frame axes to further find the different between the CC scheme and the CE scheme. Figure 4(a) shows the 3D attosecond pulse with the same parameters as the green dotted line shown in Fig. 3(a), i.e., superposing the region 390–460 eV for the case of the CC scheme. The attosecond pulse is chaotic in 3D frame axes and a satellite pulse is observed in the y direction. This implies that the phases of attosecond pulse in the x direction and in the y direction are not synchronous. For the case of the CE scheme, Fig. 4(b) shows the case of superposing 420–490 eV, and a linear polarization IAP pulse is obtained. In fact, linear polarization IAP pulses with durations of sub-60 as can be obtained by superposing 70 eV in other regions of plateau. From the above discussion, we know that the CE scheme can obtain linear polarization IAP pulses directly by superposing a bandwidth of 70 eV in the plateau area while the CC scheme cannot.

In conclusion, we have investigated the IAP generation via the CC scheme and the CE scheme by solving the two-dimensional Schrödinger equation. Both the harmonic spectra in the two schemes include the water window region. The CE scheme can obtain a longer plateau than the CC scheme with the same intensity. From the time-frequency analysis, the short quantum path in peak B_2 is controlled for the case of $\varepsilon = 0.7$, while a very weak intensity of short quantum path appears in peak B_1 for the case of the CC scheme. By superposing a bandwidth of 70 eV, an IAP with a duration of sub-60 as can be obtained and the central wavelength is selectable in the water window region. The polarization of the IAP can be shown in 3D frame axes. The IAP generated from the CE scheme is linear while the IAP generated from the CC scheme is not.

References

[1] Schoun S B, Chirla R, Wheeler J et al 2014 *Phys. Rev. Lett.* **112** 153001
[2] Wu Y and Yang X X 2007 *Phys. Rev. Lett.* **98** 013601
[3] Wu Y and Yang X X 2007 *Phys. Rev.* A **76** 013832
[4] Xiong H, Si L G, Lv X Y et al 2013 *Opt. Lett.* **38** 353
[5] Krausz F and Ivanov M 2009 *Rev. Mod. Phys.* **81** 163
[6] Drescher M, Hentschel M, Kienberger R et al 2002 *Nature* **419** 803
[7] Goulielmakis E, Loh Z H, Wirth A et al 2010 *Nature* **466** 739
[8] Feng X, Gilberston S, Mashiko H et al 2009 *Phys. Rev. Lett.* **103** 183901
[9] Goulielmakis E, Schultze M, Hofsteter M et al 2008 *Science* **320** 1614
[10] Pei Y N and Miao X Y 2014 *Chin. Phys. Lett.* **31** 104202
[11] Lan P, Lu P, Li Q et al 2009 *Phys. Rev.* A **79** 043413
[12] Du H C and Hu B T 2011 *Phys. Rev.* A **84** 023817
[13] Zheng Y, Zeng Z, Li R et al 2012 *Phys. Rev.* A **85** 023410
[14] Hong W, Lu P, Li Q et al 2009 *Opt. Lett.* **34** 2102
[15] Jiao Z H, Wang G L, Li P C et al 2014 *Phys. Rev.* A **90** 025401
[16] Kienberger R, Coulielmakis E, Uiberacker M et al 2004 *Nature* **427** 817
[17] Abel M J, Pfeifer T, Nagel P M et al 2009 *Chem. Phys.* **366** 9
[18] Chang Z 2005 *Phys. Rev.* A **71** 023813
[19] Zhao S F, Zhou X X, Li P C et al 2008 *Phys. Rev.* A **78** 063404
[20] Xia C L, Zhang G T, Wu J et al 2010 *Phys. Rev.* A **81** 043420
[21] Chen J G, Zeng S L and Yang Y J 2010 *Phys. Rev.* A **82** 043401
[22] Zhao K, Zhang Q, Chini M et al 2012 *Opt. Lett.* **37** 3891
[23] Xia C L and Liu X S 2013 *Phys. Rev.* A **87** 043406
[24] Liu C D and Nisoli M 2012 *Phys. Rev.* A **85** 013418
[25] Ruiz C, Hoffmann D J, Torres R et al 2009 *New J. Phys.* **11** 113045
[26] Du H C, Xue S, Wang H Q et al 2015 *Opt. Commun.* **338** 422
[27] Hernández-García C, Pérez-Hernández J, Popmintchev T et al 2013 *Phys. Rev. Lett.* **111** 033002